

SUPPORTING INFORMATION

Boron-containing fullerene based salts with cyclic carbonate solvents as electrolytes for Li-ion battery and beyond

Piyusaranjan Giri, Sourab Barath V, Shakuntala Dhurua, Sankar Maity, Rabiul
Gazi, and Madhurima Jana*

*Molecular Simulation Laboratory, Department of Chemistry, National
Institute of Technology, Rourkela - 769008, India*

*To whom correspondence should be addressed. E-mail: janam@nitrkl.ac.in

1. Molecular Dynamics simulation method using Reactive force field

Reactive molecular dynamics simulations were performed using LAMMPS¹ molecular dynamics package using the ReaxFF^{2,3} force field. Two distinct systems, containing LiBF₄/EC and LiC₅₉B/EC were prepared to study the effects of the salts on the decomposition of the solvent. All the model systems consist of 13LiBF₄ / LiC₅₉B molecules solvated in 577EC molecules in a simulation box of dimensions 4.0 × 4.0 × 4.0 nm³. The TopoTools⁴ plugin bundled with VMD⁵ was used to read the initial configuration generated by Packmol and assign partial charges to all the atoms in the system and save a data file compatible with LAMMPS. The simulations were conducted using the ReaxFF force field generated and validated by Islam M and coworkers⁶. To eliminate initial stress, all the systems were first minimized using the conjugate gradient minimization algorithm as implemented in the LAMMPS code. In order to equilibrate the system and ensure the steady state diffusion of the system, without any reactions taking place, the system was rescaled to 50 K over 10 ps using the Nosé-Hoover thermostat⁷ barostat, with the Parinello-Rahman barostat method⁸ to maintain 1.0 bar of pressure. Thereafter, systems were equilibrated at 50 K for another 10 ps using the NVT ensemble. Following this, the systems were rescaled for 50 ps using a time step of 0.25 fs, under the NVT ensemble, in order to accelerate the reaction kinetics. This is a common procedure used in other studies as well⁹. The systems were then further equilibrated for 50 ps. Production runs were then performed using the appropriately rescaled and equilibrated system using an integrator time step of 0.25 fs for 200 ps. The trajectory and species information obtained from the production runs were analysed using

OVITO¹⁰ and a home grown script to study the various decomposition products of ethylene carbonate and the ions.

Table S1: Number of anions around cation in the first coordination shell as obtained from the running coordination number calculated from $g(r)$.

Systems	N	
	EC	PC
LiBF ₄	3.203	2.915
NaBF ₄	3.040	3.193
Mg(BF ₄) ₂	3.663	3.934
LiC ₅₉ B	1.162	1.732
NaC ₅₉ B	1.171	1.210
MgC ₅₈ B ₂	0.071	0.219

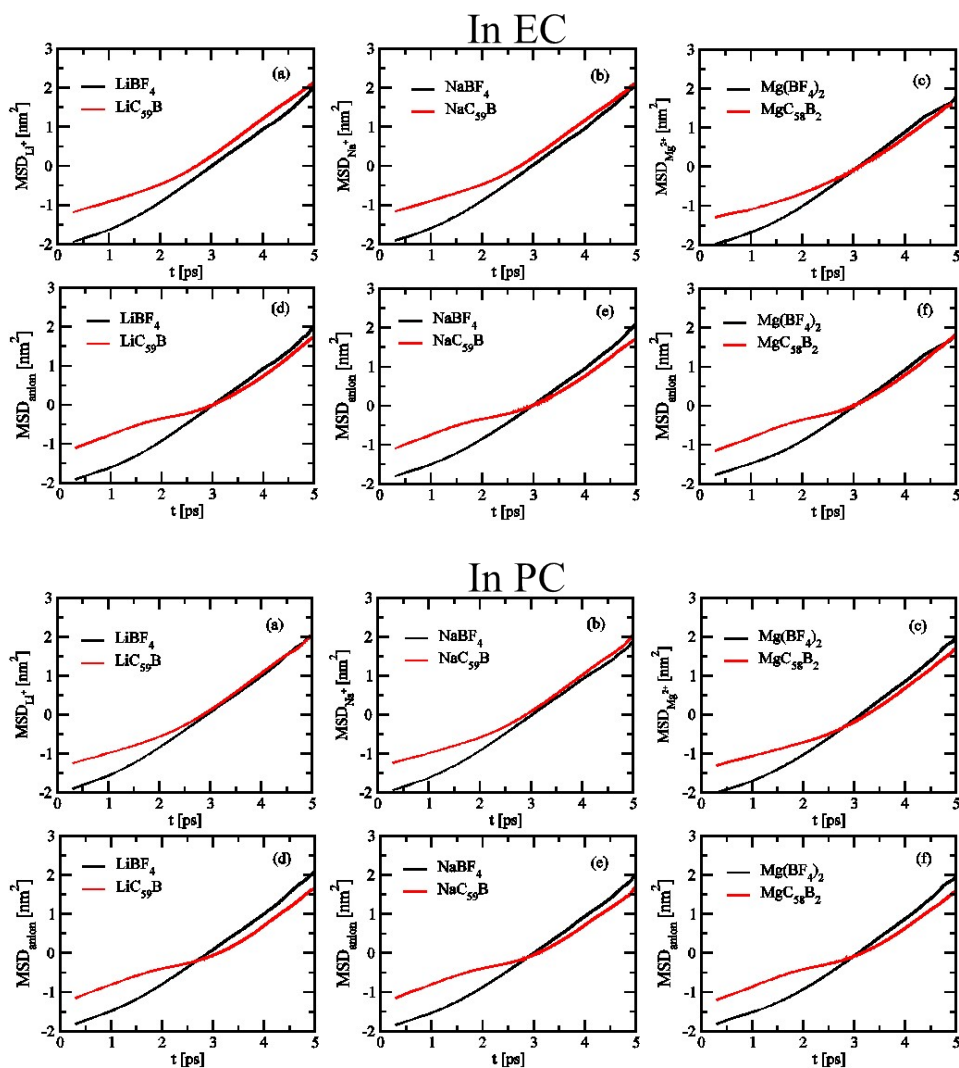


Figure S1: The log-log plots of the translational mobility of cations (a,b,c) and anions (d,e,f) in EC and PC solvent.

Transverse current correlation function:

The transverse current correlation function was calculated from Gromacs, that follows the approach described by Bruce J. Palmer.¹¹ The details of the method can be found elsewhere.¹¹ According to the method, microscopically, the discrete particles of fluid are always executing random thermal motion, even in equilibrium. A microscopic definition for the transverse momentum fields can be expressed as

$$\mu_y^{micro}(x,t) = \sum_{j=1}^N p_y^j(t) \delta(x - x^j(t)) \dots\dots\dots(1)$$

For periodic systems the Fourier coefficient expressed as,

$$\mu_y^{micro}(k_x,t) = \sum_{j=1}^N p_y^j(t) e^{-ik_x x^j(t)} \dots\dots\dots(2)$$

To extract the long-time decay behavior of $\mu_y^{micro}(k_x,t)$, the transverse-current autocorrelation function $C_{\perp}(k_x,t)$ is formed from the microscopic Fourier coefficients via following expression,

$$C_{\perp}(k_x,t) = \langle \mu_y^{micro}(k_x,t) \mu_y^{micro}(k_x,0) \rangle \dots\dots\dots(3)$$

where the angular brackets indicate an equilibrium average over initial conditions. If k_x is sufficiently small and t is sufficiently large, then $C_{\perp}(k_x,t)$ should decay as,

$$C_{\perp}(k_x,t) \sim e^{-(\mu k_x^2/\rho)t} \dots\dots\dots(4)$$

To calculate transverse current auto correlation function in actual practice, it is convenient to use the following expression instead of eq 2,

$$u_{\square}^{micro}(k, t) = \sum_{j=1}^N \hat{k}_{\square} p^j(t) \sin_{\square}[k \cdot r^j(t)] \dots\dots\dots(5)$$

$$u_{\square}^{micro}(k, t) = \sum_{j=1}^N \hat{k}_{\square} p^j(t) \cos_{\square}[k \cdot r^j(t)] \dots\dots\dots(6)$$

In the small- k limit both the atomic and molecular definitions give the same $u_{\square}^{micro}(k, t)$ and $C_{\perp}(k_x,t)$. For finite k , the molecular definition of $u_{\square}^{micro}(k, t)$ appears to give smoother C_{\perp}

$k_x(t)$ at short times. The vector \hat{k}_{\square} is defined as a unit vector perpendicular to the vector \mathbf{k} . For any \mathbf{k} , it is possible to construct two orthogonal \hat{k}_{\square} 's. The allowable values of \mathbf{k} are

$$k = \frac{2\pi}{L}(n_1, n_2, n_3) \dots\dots\dots(7)$$

where n_1, n_2, n_3 are integers. The procedure follows the crystallographic convention of labeling all equivalent \mathbf{k} vectors.

Table S2: The diffusion co-efficient values of cation and anion and cation transport number of LiC_{59}B /EC system at all the studied temperatures.

System LiC_{59}B (K)	$D_{\text{M}^+} (\times 10^{-6} \text{ cm}^2/\text{s})$	$D_{\text{A}^-} (\times 10^{-6} \text{ cm}^2/\text{s})$	t_+
278	0.72	1.19	0.37
288	0.80	1.09	0.42
298	1.18	1.23	0.48
308	1.60	1.22	0.56
318	1.90	1.13	0.62
330	2.76	1.37	0.66
340	3.45	1.73	0.66

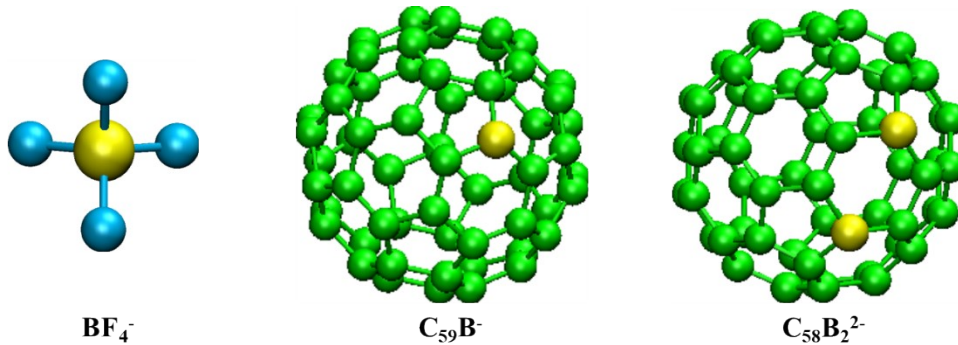


Figure S2: Optimized geometries of BF_4^- , C_{59}B^- and $\text{C}_{58}\text{B}_2^{2-}$.

Table S3: Diffusion co-efficient of cation without and with the electric field (1.5V nm^{-1})

System	$D_+ (10^{-6} \text{ cm}^2/\text{s})$	$D_+ (10^{-4} \text{ cm}^2/\text{s})$
	Without electric field	With electric field
$\text{LiC}_{59}\text{B-EC}$	2.76	2.92
$\text{NaC}_{59}\text{B-EC}$	2.64	4.42
$\text{MgC}_{58}\text{B}_2\text{-EC}$	1.42	4.19

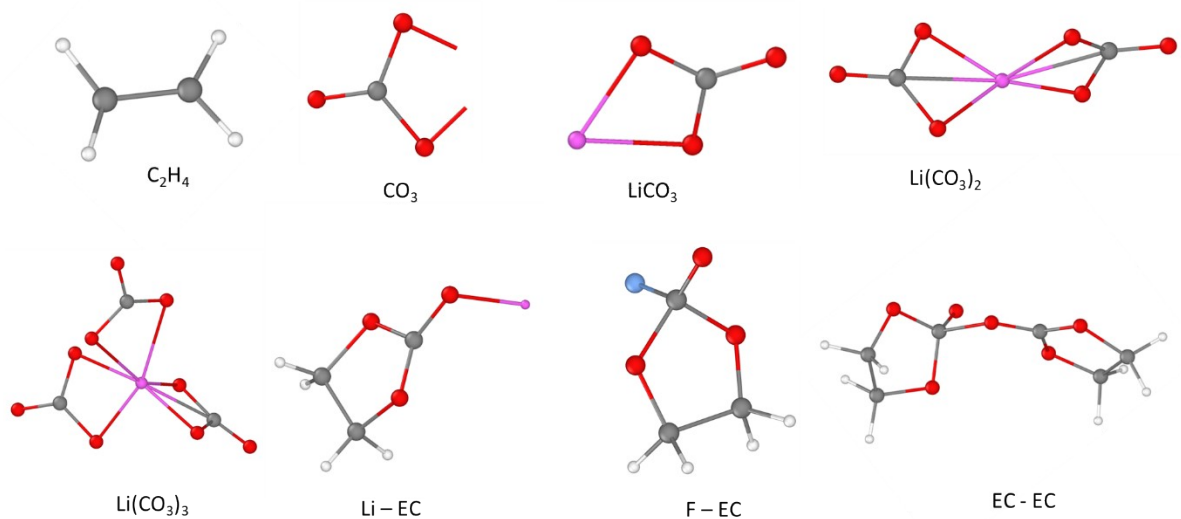


Figure S3: Structure of different intermediates as obtained from the ReaxFF simulations

Reference

1. A. P. Thompson, H. M. Aktulga, R. Berger, D. S. Bolintineanu, W. M. Brown, P. S. Crozier, P. J. in 't Veld, A. Kohlmeyer, S. G. Moore, T. D. Nguyen, R. Shan, M. J. Stevens, J. Tranchida, C. Trott and S. J. Plimpton, *Computer Physics Communications* 2022, **271**, 108171.
2. A. C. T. Van Duin, S. Dasgupta, F. Lorant and W. A. Goddard, *J. Phys. Chem. A* 2001, **105**, 9396–9409.
3. H. M. Aktulga, J. C. Fogarty, S. A. Pandit and A. Y. Grama, *Parallel Comput.* 2012, **38**, 245–259.
4. A. Kohlmeyer and J. Vermaas, 2022. TopoTools: Release 1.9.
5. W. Humphrey, A. Dalke and K. Schulten, *Journal of Molecular Graphics* 1996, **14**, 33–38.
6. M. M. Islam, V. S. Bryantsev and A. C. T. van Duin, *Journal of The Electrochemical Society* 2014, **161**, E3009–E3014.
7. G. J. Martyna, M. E. Tuckerman, D. J. Tobias and M. L. Klein, *Mol. Phys.* 1996, **87**, 1117–1157.
8. M. Parrinello and A. Rahman, *J. Appl. Phys.* 1981, **52**, 7182–7190.
9. D. Bedrov, G. D. Smith and A. C. T. van Duin, *The Journal of Physical Chemistry A* 2012, **116**, 2978–2985.
10. A. Stukowski, *Modelling and Simulation in Materials Science and Engineering* 2009, **18**, 015012.
11. B. J. Palmer, *Phys. Rev. E* 1994, **49**, 359.

